

Supercapacitor efficiency of controlled hydrothermally synthesized ZnO and CeO₂-ZnO nanocomposites: investigation and performance analysis

S. R. Shafqat ^a, S. Riaz ^a, R. Jabbar ^a, S. Sajid ^a, S. Khawar ^a, Z. A. Sandhu ^b,
M. Danish ^{a,*}, M. S. Youssef ^c, H. T. Ali ^c, M. A. Raza ^b

^a *Department of Chemistry, Faculty of Science, University of Sialkot, Sialkot, 51310, Pakistan*

^b *Department of Chemistry, Faculty of Science, University of Gujrat, Hafiz Hayat Campus, Gujrat, 50700, Pakistan*

^c *Department of Mechanical Engineering, College of Engineering, Taif University, Kingdom of Saudi Arabia*

Researchers are concerning critical energy crisis and environmental deterioration due to excessive use of non-renewable energy resources. An in-depth study has visualized that the synthesis of Cerium-based ZnO nanocomposite plays pivot role in the success of energy storage devices. In this regard, a one-pot hydrothermal approach was employed for the successful synthesis of pure ZnO and CeO₂-ZnO nanomaterials. The prepared materials were assessed with electrochemical performance and recommending that this composite material is showing remarkable capacitive and energy density performance. The scanning electron microscope exhibited interparticle interaction of zinc and cerium material enhanced Supercapacitor performance of material. The higher intensity peak at 525 cm⁻¹ corresponds to the Ce-O stretching mode that ensures the synthesis of the cerium oxide nanoparticles. The cyclic voltammetry showed excellent specific capacitance of 1031 F/g for CeO₂-ZnO composite material. Similarly, the composite material also illustrated excellent energy density value of 36.24 Wh/kg. Lastly, the electrochemical impedance spectroscopy exhibited lower electrolyte-electrode resistance at the interface that suggest better electrochemical performance of composite material and recommending material in energy storage system.

(Received July 10, 2025; Accepted September 30, 2025)

Keywords: Nanomaterials, Hydrothermal, Energy crises, Binary composites, Super capacitor

1. Introduction

Energy being one of the important constituent of modern life, with the ever growing population of globe with recent developments in technology [1]. With the increment in energy demand, a higher concern has been govern at the fuel-based generation systems as a convenient solution, but such systems have adverse harmful effects on environment and the ecology [2]. These sources bring high emission of greenhouse gases, cause climatic changes and environmental degradation. In this regards, the use of fossil fuel is not sustainable and there is dire need to shift to other cleaner, more certain and eco-friendly energy sources [3]. To address these challenges, researchers are focused on renewable sources like solar energy, wind power, hydrogen energy, and lithium ion battery technology have come into light as great alternatives [4]. The advantage of these energy sources are that they do not only lower dependence on fossil fuels, but are also less harmful for environment [5]. Their effectiveness and efficiency mainly depend on development of the advanced storage systems of energy to store and supply it with reliability in terms of energy supply-demand misalignments [6]. Conventional batteries and capacitors are considered as most convenient energy storage devices as compared to conventional materials. Batteries are mostly characterized by high energy density and weak power density with shorter life cycles [7]. However, capacitors can

* Corresponding authors: drdanish62@gmail.com
<https://doi.org/10.15251/JOR.2025.215.619>

provide large power and still have a small amount of energy stored. Such constraints have triggered the emergence of the importance of other storage devices, which can help fill the power-energy performance gap [8].

Supercapacitor has proven to be one of the most promising solutions and has had immensely great benefits over the conventional ones. They have high power density, fast charge-discharge, long based cycling, and low maintenance [9].

In this way, Supercapacitor have shown versatility in various applications, including portable electronics, electric vehicles and back-up power systems [10]. Supercapacitor can be broadly classified into two- electrical double-layer capacitors (EDLCs), and pseudocapacitors depending on their mechanisms of charge storage [11]. EDLCs are generally made by means of carbon electrodes, e.g. activated carbon, graphene and carbon nanotubes, through which energy is stored via accumulation of electrostatic charges at the electrode-electrolyte interface [12]. Now a day, metal-oxide nanomaterials are efficiently use as efficient electrode materials in EDLC [13]. Conversely, pseudocapacitors are based upon the rapid and reversible Faradaic redox reactions between the electrolyte surface and electroactive materials (typically metal oxides or conducting polymers) leading to increased specific capacitance [14]. Oxides of transition metals (TMOs) have particularly received the interest because of their potential to undergo repeated redox conversions. This facilitates effective storage of charge and this makes them very useful in Supercapacitor and pseudocapacitors [15].

Cerium oxide (CeO_2), among others, is a very promising potential TMO, because of the ease with which it can undergo the switching process between oxidation states Ce^{3+} and Ce^{4+} . This binary or dual transition contributes to rapid reversible redox reactions, which cause a high capacitive behaviour. CeO_2 is also not toxic, recyclable and chemically stable. However, this has inherently a pore conductivity and this may restrict its performance [16, 17]. Zinc oxide (ZnO) is another significant TMO that has high electron mobility, excellent electrical conductivity and chemical stability. It is widespread, non-toxic and non-hazardous, therefore, it can be used in large scale. ZnO when used in conjunction with CeO_2 improves structural stability and electron transfer [18, 19]. One pot hydrothermal synthesis of nanomaterials is considered more appropriate approach. This technique is well known due to its numerous benefits which are appropriate temperature processing, composition control, high purity, homogeneous and porous nanostructures production [20].

Obodo et al., has recently conducted research on electrode materials based on cerium oxide (CeO_2), zinc oxide (ZnO) and their composite $\text{CeO}_2 @ \text{ZnO}$ were prepared by the use of a green hydrothermal methodology involving the utilization of an organic complexing agent (*Sarcophrynium Brachystachys* leaf extract). Electrochemical properties evaluated using cyclic voltammetry (CV) at a scan rate of 10.0 mV/s showed specific capacitance of 976 F/g, 878 F/g and 1075 F/g of $\text{CeO}_2 @ \text{ZnO}$ and the composite respectively [18]. The present work synthesized CeO_2 - ZnO nanocomposite via one-pot hydrothermal methodology. The prepared composite show valuable synergistic effect that can be explore in distinct characterizations techniques. The refine morphology of SEM analysis and XRD confirm the successful incorporation of cerium into ZnO matrix. Moreover, this study depicted excellent capacitive performance and cycling excellence of composite electrode material.

2. Experimental work

2.1. Material used

The pure ZnO and CeO_2 - ZnO nanocomposite was synthesized utilizing distinct precursor salts of zinc and cerium metal. The zinc acetate dihydrate ($\text{Zn}(\text{CH}_3\text{COO})_2 \cdot 2\text{H}_2\text{O}$) and cerium sulphate tetrahydrate ($\text{CeSO}_4 \cdot 4\text{H}_2\text{O}$) precursor slats used with 99.99% purity. All the metal precursor salts were purchased from sigma Aldrich. The ethanol was employed as a solvent during the preparation of slurry for working electrode. All the materials used during synthesis as purchased without any further modification.

2.2. Synthesis of pure CeO₂ nanomaterial

The pure ZnO and CeO₂-ZnO Nanocomposites binary composite material was synthesized through one-pot hydrothermal synthesis methodology. The cerium sulphate tetrahydrate (CeSO₄·4H₂O), zinc acetate dihydrate (Zn(CH₃COO)₂·2H₂O) and specific amount of urea were taken as precursors salts in the synthesis mechanism. All the metal salts and urea were incorporated in the deionized water and allowed to perform consistent homogenization of metal salts at 600-650 rpm. The homogenized solution mixture than added into a Teflon-lined stainless-steel autoclave. The autoclave was tightened and placed in oven at 140 °C for 4 h. After hydrothermal treatment of specific time, the autoclave placed out from oven and let them cool at room temperature. The cooled solution then washed with absolute ethanol and distilled water for purification and remove unnecessary impurities. The washed solution precipitate was later dried at 60°C for night. The dried powder material undergoes further calcination process for more refined and uniform morphology at 350°C for 3-4 h in furnace. This hydrothermal approach exhibited higher degree of crystallinity, defined shape and size of composite material. provided medium for defined size, shape, and degree of crystallinity of composites materials.

3. Results and discussion

3.1. Characterization

The compositional and functional group analysis of synthesized nanoparticles was investigated by Fourier transform infrared spectroscopy (FTIR). The FTIR spectrum of CeO₂-ZnO nanocomposite is shown in figure 1. The higher intensity peak at 525 cm⁻¹ [21, 22] has been attributed to the Ce-O stretching mode that evidences the presence of the cerium oxide nanoparticles. Similarly, other bands at 673 cm⁻¹ [23, 24] and 998 cm⁻¹ [25], are also attributed to CeO₂ lattice vibrations and oxygen-metal stretching of the fluorite like structure, indicating good crystallinity and bonding in the CeO₂ phase. Meanwhile, the sharp signals at 588 cm⁻¹ [26, 27], 1053 cm⁻¹ [28, 29] and 1165 cm⁻¹ [27] are related to Zn-O stretching vibrations and are typical of zinc oxide nanoparticle. The indication of ZnO within the composite which was confirmed by these bands representing the vibrational energy levels of Zn-O bond usually seen in a wurtzite structure. The clear differentiation of the cerium and zinc associated peaks and their clearness testify good synthesis and excellent interaction at the nano level. The lack of peaks related to organic contaminants indicates good purity of the nanocomposite and the sharpness of bands in the fingerprint range demonstrates structure integrity of metal oxide framework.

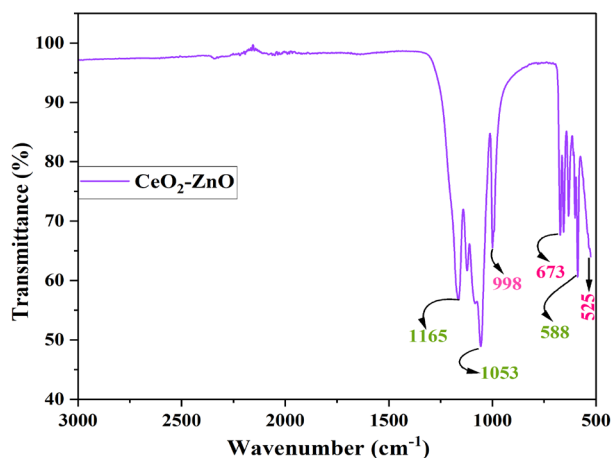


Fig. 1. FTIR analysis of CeO₂-ZnO binary nanocomposites.

The X-ray diffraction spectroscopy (XRD) analysis was performed to find out structural composition, phase purity and crystalline phases of fabricated CeO_2 -ZnO nanocomposite. The pink marked peaks represent cerium oxide and are indexed corresponding to cubic fluorite phase of CeO_2 which is aligned with the JCPDS card # 00-001-0800 [30, 31]. Reflections at planes 25° (100), 27° (111), 31° (200), 48° (220), 52° (102), 56° (311), 58° (222) and 69° (400) are sharp, which represents a well-trodden cubic structure of CeO_2 . Meanwhile, the green-marked peaks are zinc oxide and assigned index to the hexagonal wurtzite structure according to JCPDS card # 01-075-1526 [32-34]. The observations of 29° (100), 34° (002), 36° (101), 47° (102), 63° (103), 66° (200) and 71° (004) confirm ZnO crystallinity and phase purity. The existence of crystallite peak, 38° (102), that is indexed using JCPDS card no. 00-044-1086 of CeO_2 [35, 36] and 42° (200) corresponding to JCPDS # 01-077-0191 of ZnO [37, 38] is a sign of the secondary phases in the composite. These secondary phases can be caused by remaining (or unreacted) precursor material, non-stoichiometric defects or minor variations in crystallite size and structure produced in the course of synthesis. They present less intense intensities than the main phases, implying the idea that they comprise small parts. Figure 2 illustrated the XRD spectrum of composite material.

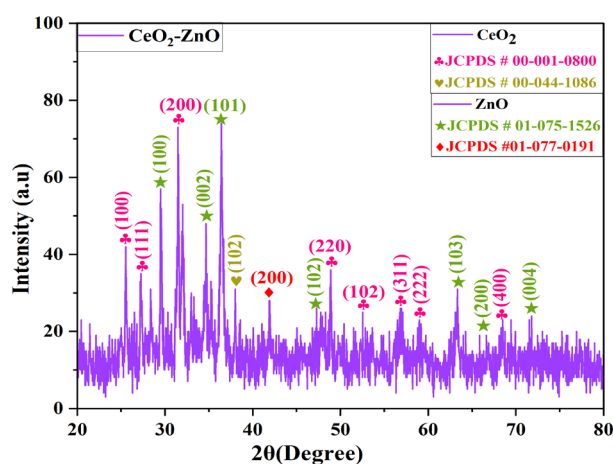


Fig. 2. XRD analysis of synthesized CeO_2 -ZnO binary nanocomposites.

The scanning electron microscope (SEM) analysis of both pure ZnO and CeO_2 -ZnO composite material is illustrated in figure 3. The pure ZnO analysis ensures the irregular shape densely packed agglomerated structures with rough surface morphology, suggesting a porous structure. Conversely, the composite material exhibited more uniform structural morphology with well-dispersed agglomerates distributed on the surface of material, showing excellent interparticles interaction and improved surface area. The enhanced structural morphology and synergistic interaction of cerium and zinc facilitate effective ion transportation and improved electrochemical performance of composite material than pure ZnO nanomaterial. This optimizes structure of composite material increase porosity and interaction between particles.

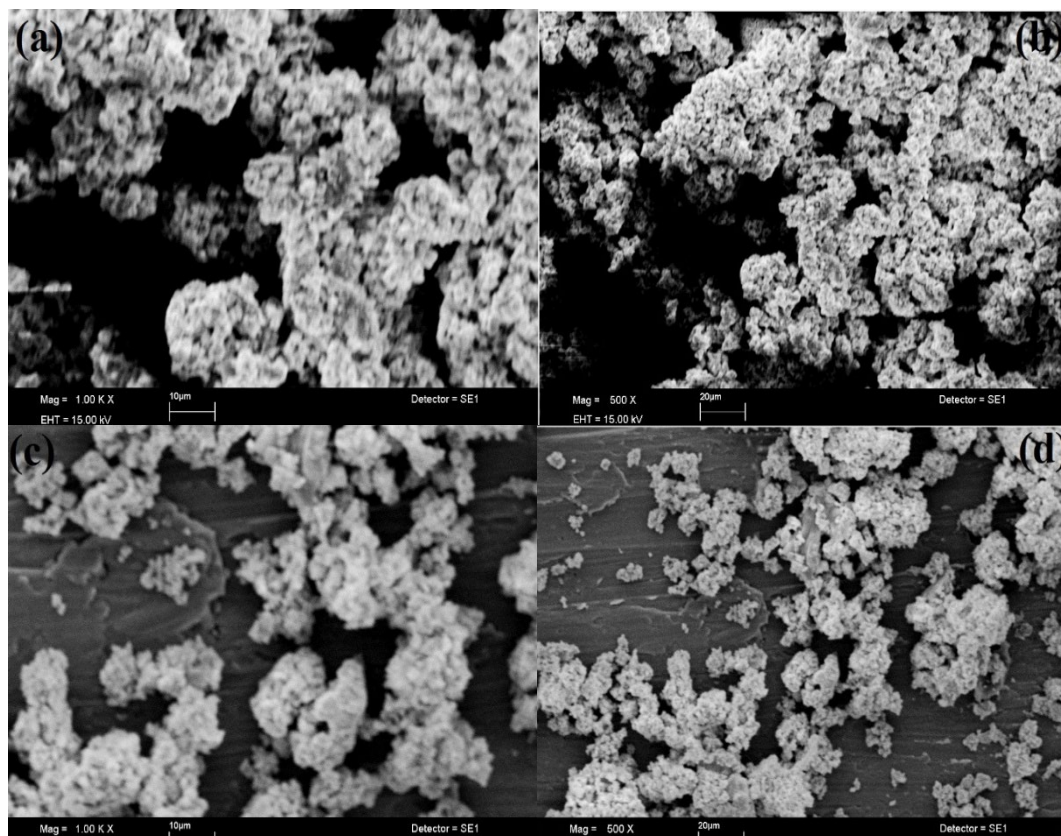


Fig. 3. SEM analysis of prepared nanomaterials, (a, b) Pure ZnO, and (c, d) CeO₂-ZnO.

3.2. Electrochemical performance of ZnO and CeO₂-ZnO nanocomposites

The electrochemical activity of pure ZnO and CeO₂-ZnO was investigated using cyclic voltammetry (CV), and electrochemical impedance spectroscopy (EIS). The CV performance was carried out at different scan rates from 10–200 mVs⁻¹ in 2M KOH electrolyte solution. It clearly showed that the pure ZnO and CeO₂-ZnO electrode material illustrated symmetrical shapes of CV, which confirms the pseudocapacitive behaviour of working electrode material. The higher integral area under curve of CeO₂-ZnO exhibited the excellent conductivity and mobility of ions [39]. The higher surface area and current response of composite electrode material ensures the better distribution of cerium ions into the matrix of ZnO nanomaterial which directly involve in decline of cation diffusion pathways in the time of electrochemical process [40]. The specific capacitance of pure ZnO and CeO₂-ZnO was calculated using reported equation 1 [5, 41].

$$C_{sp} = \frac{\int_{V_a}^{V_c} I(V) dV}{mv(V_c - V_a)} \quad (1)$$

Here m depicts about active mass of electrode material, v visualize the scan rate and $V_c - V_a$ designates to potential window.

It was observed that the increase of scan rate inversely effects the specific capacitance values of pure and composite materials. The increase in scan rate from 10-200 mVs⁻¹, a decline in specific capacitance values were observed due to restricted faradic redox mechanism on the surface of electrode as shown in figure 4 (a-b). It may also due to restricted surface area and not accessibility of active sites on the surface of electrode.

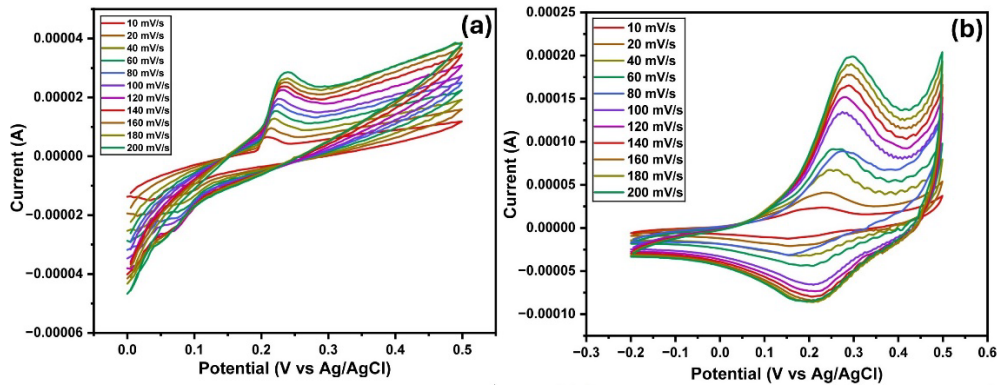


Fig. 4. Cyclic voltammetry performance of prepared nanocomposites, (a) CV curves of pure ZnO at 10-200 mVs^{-1} , (b) CV curves of $\text{CeO}_2\text{-ZnO}$ composite at 10-200 mVs^{-1}

The aforementioned equation was used to calculate the specific capacitance of pure ZnO and $\text{CeO}_2\text{-ZnO}$ was 753 and 1031 F/g, respectively. The $\text{CeO}_2\text{-ZnO}$ composite material showed superior capacitance value than pure ZnO material, owing to its higher area, maximum $I\text{-}V$ response and better conductivity.

Similarly, the energy density of nanocomposite materials were calculated using reported equation 2 [42, 43].

$$E.D = \frac{C_{sp} \times \Delta V^2 \times 1000}{2 \times 60 \times 60} \quad (2)$$

The energy density of pure ZnO and $\text{CeO}_2\text{-ZnO}$ was calculated 26.16 and 36.24 Wh/kg, respectively as shown in figure 5 (a, b).

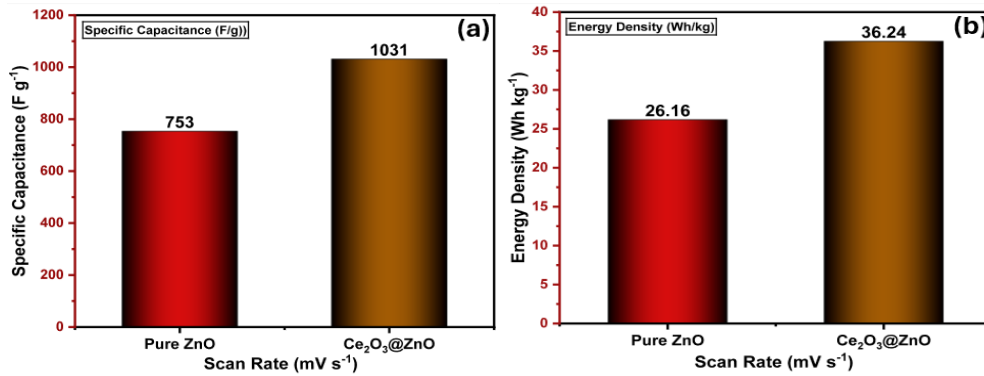


Fig. 5. Specific capacitance and energy density of pure and composite material, (a) specific capacitance of pure ZnO and $\text{CeO}_2\text{-ZnO}$, (b) energy density of pure ZnO and $\text{CeO}_2\text{-ZnO}$.

The electrochemical impedance spectroscopy is used for the evaluation of electrochemical excellence of Supercapacitor. The EIS allow to observe effect of electrical impedance with frequency for the analysis of electrochemical system. Furthermore, it also provides information about interactions involves between electrolytes and electrodes [44]. It is shown by a Nyquist plot consisted of two regions, a straight line and a semicircle region. The Nyquist plot was drawn between real impedance and imaginary impedance. A small semicircle was observed for $\text{CeO}_2\text{-ZnO}$ at high frequency region, specifies the capacitive nature of composite electrode material. Similarly, no semicircle or a straight line was observed in case of pure ZnO nanomaterial that may be due to non-uniform electric field at the electrode interface or rough electrode surface [17]. The Equivalent

Series Resistance (ESR) of pure ZnO and CeO₂-ZnO composite material as shown in figure 6. The ESR illustrates the combine effect of electrode/electrolyte interface resistance, solution resistance and electrodes resistance. The CeO₂-ZnO composite electrode material visualized lower resistance than pre ZnO, indicating highly conductive material that have been also assessed with cyclic voltammetry results. Similarly, ZnO showed higher resistance and recommended as less conductive material for supercapacitor performance [18].

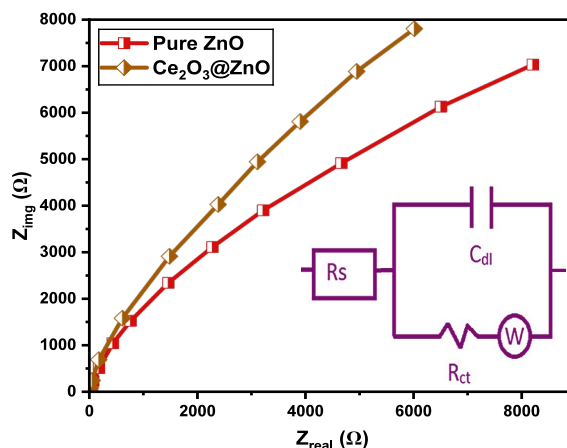


Fig. 6. Electrochemical impedance spectroscopy and equivalent series resistance representation of pure ZnO and CeO₂-ZnO

4. Conclusion

In this study, Zinc-based transition metal oxides were prepared through hydrothermal technique. The prepared material showed well defined interconnected synergistic interaction between both metals in composite material. The pure and composite material assessed with cyclic voltammetry and electrochemical impedance spectroscopy for the determination of faradic redox and ions kinetic mechanism respectively. The CV analysis confirmed effective charge storage mechanism in composite material with excellent capacitive performance of 1031 F/g higher than pure 753 F/g. The enhanced surface area and improved active site on the surface of composite electrode material increase transportation of charges that ensure lower resistance between electrode and electrolyte. Additionally, the energy density for both materials were calculated about 36.24 Wh/kg and 26.16 Wh/kg, for CeO₂-ZnO and ZnO composite material, respectively. Finally, the composite material plays remarkable role in the fulfil demand of energy crisis in with excellent energy storage and conversion capacity.

Acknowledgements

The authors would like to acknowledge Deanship of Graduate Studies and Scientific Research, Taif University for funding this work.

References

- [1] G. Paul, M. Prakash, IGI Global2025, pp. 351-368
- [2] S. Yang, Y. Fu, Energy Economics (2025) 108290;
<https://doi.org/10.1016/j.eneco.2025.108290>

- [3] R. Anjana, P. Anjana, J. Alex, R. Isaac, R.S. Hussain, D. Sajan, *Diamond and Related Materials* 146 (2024) 111241; <https://doi.org/10.1016/j.diamond.2024.111241>
- [4] A.K. Sarker, A.K. Azad, M.G. Rasul, A.T. Doppalapudi, *Energies* 16(3) (2023) 1556; <https://doi.org/10.3390/en16031556>
- [5] Z.A. Sandhu, Asifa, S.R. Shafqat, M. Danish, K.M. Batoo, M.F. Ijaz, M.A. Raza, S. Ashraf, S. Ghaffar, *Ionics* (2025) 1-16; <https://doi.org/10.1007/s11581-025-06267-4>
- [6] S. Hussnain, M.R. Khawar, H.T.H. Rana, N.A. Shad, M.K. Abbas, M.D. Albaqami, A. Ahmad, S. Cho, Y. Javed, D. Choi, *Materials Science in Semiconductor Processing* 192 (2025) 109412; <https://doi.org/10.1016/j.mssp.2025.109412>
- [7] A.G. Olabi, Q. Abbas, A. Al Makky, M.A. Abdelkareem, *Energy* 248 (2022) 123617; <https://doi.org/10.1016/j.energy.2022.123617>
- [8] A. Aldayyat, F.K. Yam, *Journal of Solid State Electrochemistry* (2025) 1-32; <https://doi.org/10.1007/s10008-025-06280-7>
- [9] S. Vennila, C. Leelavathi, V. Balaprakash, K. Thangavel, S.A. Kumar, J.K. Sundar, R. Ramesh, *Journal of Materials Science: Materials in Electronics* 36(8) (2025) 489; <https://doi.org/10.1007/s10854-025-14579-4>
- [10] K.O. Oyedotun, J.O. Ighalo, J.F. Amaku, C. Olisah, A.O. Adeola, K.O. Iwuozor, K.G. Akpomie, J. Conradie, K.A. Adegoke, *Journal of Electronic Materials* 52(1) (2023) 96-129; <https://doi.org/10.1007/s11664-022-09987-9>
- [11] D. Bejjanki, S.K. Puttapati, *Multidimensional Nanomaterials for Supercapacitors: Next Generation Energy Storage*, Bentham Science Publishers 2024, pp. 29-48; <https://doi.org/10.2174/9789815223408124010004>
- [12] R. Dubey, V. Guruviah, *Ionics* 25 (2019) 1419-1445; <https://doi.org/10.1007/s11581-019-02874-0>
- [13] I. Shaheen, K.S. Ahmad, C. Zequine, R.K. Gupta, A.G. Thomas, M.A. Malik, *RSC Advances* 11(38) (2021) 23374-23384; <https://doi.org/10.1039/D1RA04341B>
- [14] P. Bhojane, *Journal of Energy Storage* 45 (2022) 103654; <https://doi.org/10.1016/j.est.2021.103654>
- [15] A. Nicholson, P.R. Kumar, F. Kamarulazam, M. Pershaanaa, K. Ramesh, S. Ramesh, *Ionics* 31(5) (2025) 4885-4900; <https://doi.org/10.1007/s11581-025-06215-2>
- [16] M. Mazloun-Ardakani, F. Sabaghian, M. Yavari, A. Ebady, N. Sahraie, *Journal of Alloys and Compounds* 819 (2020) 152949; <https://doi.org/10.1016/j.jallcom.2019.152949>
- [17] M.R. Khawar, N.A. Shad, S. Hussain, Y. Javed, M.M. Sajid, A. Jilani, M. Faheem, A. Asghar, *Journal of Energy Storage* 55 (2022) 105778; <https://doi.org/10.1016/j.est.2022.105778>
- [18] R.M. Obodo, H.E. Nsude, S.C. Ezike, C. Ononogbo, I. Ahmad, M. Maaza, F.I. Ezema, *Hybrid Advances* 5 (2024) 100143; <https://doi.org/10.1016/j.hybadv.2024.100143>
- [19] R.M. Obodo, H.E. Nsude, S.C. Ezike, J.N. Anosike, S.E. Ugwuanyi, C.U. Eze, M.O. Duru, U.C. Elejere, A. Diallo, I. Ahmad, *Nano-Horizons: Journal of Nanosciences and Nanotechnologies* 4 (2025) 1-26.
- [20] M. Parashar, V.K. Shukla, R. Singh, *Journal of Materials Science: Materials in Electronics* 31(5) (2020) 3729-3749; <https://doi.org/10.1007/s10854-020-02994-8>
- [21] G. Jayakumar, A. Albert Irudayaraj, A. Dhayal Raj, *Optical and Quantum Electronics* 51(9) (2019) 312; <https://doi.org/10.1007/s11082-019-2029-z>
- [22] Á.G. Aponte, M.A.L. Ramírez, Y.C. Mora, J.F. Santa Marín, R.B. Sierra, *AIMS Materials Science* 7(4) (2020).
- [23] K.S. Agrawal, V.S. Patil, A.G. Khairnar, A.M. Mahajan, *Journal of Materials Science: Materials in Electronics* 28 (2017) 12503-12508; <https://doi.org/10.1007/s10854-017-7072-6>
- [24] A. Ali, U. Garg, K.U. Khan, Y. Azim, *Journal of Polymers and the Environment* 30(10) (2022) 4435-4451; <https://doi.org/10.1007/s10924-022-02522-1>

- [25] E. Kumar, P. Selvarajan, K. Balasubramanian, *Recent Research in Science and Technology* 2(4) (2010).
- [26] V. PP, *BioNanoScience* 10(1) (2020) 112-121; <https://doi.org/10.1007/s12668-019-00698-w>
- [27] M.L. de Peres, R.d.A. Delucis, S.C. Amico, D.A. Gatto, *Nanomaterials and Nanotechnology* 9 (2019); <https://doi.org/10.1177/1847980419876201>
- [28] N. Jayarambabu, B.S. Kumari, K.V. Rao, Y. Prabhu, *Int. J. Curr. Eng. Technol* 4(5) (2014) 3411-3416.
- [29] S. Bashir, M.S. Awan, M.A. Farrukh, R. Naidu, S.A. Khan, N. Rafique, S. Ali, I. Hayat, I. Hussain, M.Z. Khan, *International Journal of Nanomedicine* 17 (2022) 4073; <https://doi.org/10.2147/IJN.S372343>
- [30] H.M. Chenari, L. Riasvand, S. Khalili, *Ceramics International* 45(11) (2019) 14223-14228; <https://doi.org/10.1016/j.ceramint.2019.04.130>
- [31] A. Ghorani-Azam, J. Mottaghipisheh, M.S. Amiri, M. Mashreghi, A. Hashemzadeh, A. Haddad-Mashadrizeh, F. Nourbakhsh, M. Nadaf, M. Qayoomian, M.E.T. Yazdi, *Frontiers in Bioscience* 27(8) (2022) 1-6; <https://doi.org/10.31083/j.fbl2708227>
- [32] S. Hussain, I. Khan, M. Ayub, A. Rasheed, *Journal of Ovonic Research* 17(6) (2021).
- [33] R.S. Sabry, A.D. Hussein, *Polymer Testing* 79 (2019) 106001; <https://doi.org/10.1016/j.polymertesting.2019.106001>
- [34] M. Achehboune, M. Khenfouch, I. Boukhoubza, L. Leontie, C. Doroftei, A. Carlescu, G. Bulai, B. Mothudi, I. Zorkani, A. Jorio, *Materials Today: Proceedings* 53 (2022) 319-323; <https://doi.org/10.1016/j.matpr.2021.04.144>
- [35] N. Mushtaq, M. Khalid, M. Younas, M. Ashiq, M. Ashir, H. Ali, Q. Mahmood, M. mana AL-Anazy, E.S. Yousef, *Materials Chemistry and Physics* 323 (2024) 129624; <https://doi.org/10.1016/j.matchemphys.2024.129624>
- [36] H. Moradi, S.A. Kulinich, W. Wunderlich, M. Ghiaci, *ChemistrySelect* 9(4) (2024) e202303246; <https://doi.org/10.1002/slct.202303246>
- [37] A. Pramanik, S. Maiti, T. Dhawa, M. Sreemany, S. Mahanty, *Materials Today energy* 9 (2018) 416-427; <https://doi.org/10.1016/j.mtener.2018.07.007>
- [38] T.A. Dontsova, O.I. Yanushevskaya, S.V. Nahirniak, A.S. Kutuzova, G.V. Krymets, P.S. Smertenko, *Journal of Chemistry* 2021(1) (2021) 9378490; <https://doi.org/10.1155/2021/9378490>
- [39] G. Manibalan, M. Rajesh Kumar, G. Murugadoss, J. Yesuraj, R. Mohan Kumar, R. Jayavel, *Journal of Materials Science: Materials in Electronics* 32 (2021) 8746-8755; <https://doi.org/10.1007/s10854-021-05546-w>
- [40] A.J. Khan, L. Gao, M. Sajjad, S. Khan, A. Mateen, A. Ghaffar, I.A. Malik, X. Liao, G. Zhao, *Inorganic Chemistry Communications* 159 (2024) 111794; <https://doi.org/10.1016/j.inoche.2023.111794>
- [41] Z.A. Sandhu, M. Danish, M. Zain, M. Aslam, K.M. Batoo, M.F. Ijaz, *Materials Chemistry and Physics* (2025) 130410; <https://doi.org/10.1016/j.matchemphys.2025.130410>
- [42] M. Danish, A. Ashraf, Z.A. Sandhu, M.A. Raza, A.H. Bhalli, A.G. Al-Sehemi, *Journal of Molecular Structure* 1294 (2023) 136296; <https://doi.org/10.1016/j.molstruc.2023.136296>
- [43] Z.A. Sandhu, M. Danish, U. Farwa, M.A. Raza, A.H. Bhalli, A. Sultan, N. Alwadai, W. Mnif, *Journal of Inorganic and Organometallic Polymers and Materials* (2025) 1-14; <https://doi.org/10.1007/s10904-025-03650-6>
- [44] M. Stefan, A.M. Rostas, A.U. Ammar, A. Güngör, E. Saritas, D. Toloman, A. Varadi, S. Macavei, L. Barbu-Tudoran, C. Leostean, *Energy & Fuels* 38(19) (2024) 19088-19099; <https://doi.org/10.1021/acs.energyfuels.4c03091>